Anal. Bioanal. Electrochem., Vol. 15, No. 3, 2023, 198-213
https://www.doi.org/10.22034/abec.2023.703901

Analytical & Bioanalytical Electrochemistry

Full Paper

Protection of C38 Steel in Acidic Solution by Eucalyptus Sidroxylon Essential Oil

L. Koursaoui,[1,3] Y. Kerroum,[2] M. Tabyaoui,[2] A. Guenbour,[2] A. Bellaouchou,[2] A. Zarrouk,[2,*] I. Warad,[4] B. Satrani,[1] M. Ghanmi,[1] EM. Aouane,[3] and A. Chaouch[3]

[1]*Laboratories of Microbiology and Chemistry of Aromatic and Medicinal Plants, Forest Research Center, BP 763, Agdal, Rabat, Morocco*
[2]*Laboratory of Materials, Nanotechnology, and Environment, Faculty of Sciences, Mohammed V University in Rabat, 4 Av. Ibn Battouta, B.P 1014 Rabat, Morocco*
[3]*Biotechnology, Environment and Quality Laboratory, Faculty of Science, Ibn-Tofail University, BP 133, Kenitra, 14000, Morocco*
[4]*Department of Chemistry, AN-Najah National University, P.O. Box 7, Nablus, Palestine*

*Corresponding Author, Tel.: +212665201397
E-Mail: azarrouk@gmail.com

Received: 2 January 2023 / Received in revised form: 17 March 2023 / Accepted: 21 March 2023 / Published online: 31 March 2023

Abstract- Eucalyptus essential oil offers numerous benefits for the immune system through its antioxidant constituents. In this investigation, we attempted to explore another field of application, in which we exploit the corrosion inhibition potential of Eucalyptus Sideroxylon (ES) essential oil to protect C38 steel in an acidic solution of HCl. To uncover the facts, careful research was designed using fundamental measurements of gravimetric and electrochemical techniques, combined with scanning electron microscopy and energy dispersive spectroscopy analysis. The finding measurements showed that ES reduces the rate of corrosion that shows up on polarization curves as a mixed inhibitor. Furthermore, the impedance data acquisition revealed that the amount of charge transfer resistance has a high value when the ES concentration increases, we found 169.40 Ω cm^2 for 2.4 g/L of ES giving an efficiency of 80%. Moreover, the thermodynamic parameters showed that the interaction of ES with the metal surface is endothermic, characterized by physical adsorption.

Keywords- Eucalyptus essential oil; C38 steel corrosion; HCl; Electrochemical techniques; SEM/EDX

1. INTRODUCTION

To minimize the corrosion of metals, many methods of protection are used such as cathodic protection and anti-corrosion coating, and corrosion inhibitors, in all situations, the correct techniques require knowledge of the management of technical considerations and economics. Recently, corrosion inhibitors as a method of protection can provide and solve complicated problems that need to be considered or avoided when making a corrosion protection plan application. In addition, the application of corrosion inhibitor is a typical and intelligent method, a chemical compound can be added to any physical state of the environment, liquid, gas, or solid, to inhibit metal dissolution, but the appropriate conditions are important for the success of an inhibitor. According to Damborenea, the nature of the metals and corrosive environments can affect the effectiveness of the inhibitor [1]. Fortunately, there are many types and classes of corrosion inhibitors that help achieve this goal, including economic and environmental aspects .

Furthermore, it has recently been observed that almost all of the regulatory communities insist that the concept of environmentally friendly chemical compounds must include sustainable development as well as the protection of the environment and human health [1].
The adsorption of organic molecules that contain heteroatoms like phosphorus, nitrogen, or sulfur, which are good corrosion inhibitors, is influenced by a variety of factors, including the electronic structure of the inhibitor molecules, steric influence, aromaticity, and electron density at the donor site [2–9]. The inhibitor's surface area and molecule size. Adsorption, which results in the formation of a protective coating on the metal surface, is the mechanism behind the inhibitory process of these compounds. The use of inhibitors produced from pharmaceutical medications during the corrosive pickling process is one of the most efficient ways to stop metal from corroding in acidic conditions because of its biodegradability, environmental friendliness, low cost, and availability [10].

Either way, essential oils are part of this tendency; many researchers have reported the effectiveness of essential oils as corrosion inhibitors and reducers of bacteria activity [11–16]. Idouhli and his co-authors studied different families of Senecio anteuphorbium L as corrosion inhibitors for S300 steel in an acidic environment, and the efficiency of inhibition reached values between 75% and 90% [17]. Another study was published on the inhibition of copper in an acid medium containing NaCl, which indicated an inhibition efficiency of 89% [18]. Chraka chose a brass alloy to study its corrosion behaviors in NaCl solution using the essential oil of Ammi visnaga (L.) lam, the results showed an efficiency between 86% and 96.36% [19]. As can be seen, essential oils have inhibition efficiency depending on the medium and the metal nature.

However, it is essential to discuss the cost-effectiveness aspect of using essential oil as an anti-corrosion method. Generally; the cost-effectiveness of using corrosion inhibitors as an anti-corrosion method depends on various factors such as the type of inhibitor used, the surface

area to be protected, and the environmental conditions to which the protected surface will be exposed. Compared to other corrosion inhibitors, essential oils are relatively inexpensive. They are also easy to apply and require minimal preparation before application. However, the use of essential oil as an anti-corrosion material may be suitable for short-term protection or for surfaces that are not exposed to harsh environmental conditions.

Moreover, the effectiveness of such an inhibitor is associated with other mechanisms and factors, basically that a competitive inhibition can develop causing a positive or negative effect; this is related to the chemical compositions of the essential oil. For this, we collaborated with different laboratories to study eucalyptus essential oil as a corrosion inhibitor using two different types. In our previous study [20], we studied the corrosion inhibitor of Eucalyptus Botryoides essential oil in 1 M HCl, and this article completes our research by studying the inhibitory effect of Eucalyptus Sideroxylon in the same medium and for the same metal using various technologies and methods.

2. EXPERIMENTAL METHODS

2.1. Extraction of essential oil

Eucalyptus Sideroxylon (ES) Essential Oil was fabricated using the hydrodistillation method, the preparation procedure and the identification of the chemical composition by GC and GC/MS has been described in detail in our previous work [20], and the results of the chemical compositions are listed in Table 1.

2.2. Materials

The mixture of chemical elements that constitutes the C38 steel are 0.034% S, 0.165% Si, 0.179% C, 0.203% Cu, 0.439% Mn, and Fe balance. The substrates were typically prepared to ensure that the surface area is 1 cm^2, a rough surface was polished with emery paper, and the grade of 180 up to 1200 was used, the cleaning procedure for the samples was achieved by distilled water and acetone.

2.3. Preparation of the solutions

Aggressive environments in the presence of different masses of ES were obtained by preparing 1M HCl solutions. Experiments were performed in the absence of ES (blank solution) and the presence of ES.

2.4. Electrochemical measurements

To measure the electrochemical properties, the electrochemical cell of three electrodes was used, C38 steel substrates as the working electrode, and platinum metal as the counter electrode, potential of the working electrode was measured through the saturated calomel

electrode (SCE), and all experimental testing procedures were performed using the PGZ 301 (Radiometer Analytical) potentiostat driven by VoltaMaster 4 software. The corrosion process was accelerated utilizing the Potentiodynamic Polarization (PDP) parameters of 1 mV/s and the potential deviation from -600 to -200 mV/SCE. On the other hand, the impedance of the metal in each experiment is plotted according to the electrochemical impedance spectroscopy (EIS) parameters of 10 mV peak to peak, with an interval of frequencies (100 kHz to 10 mHz).

Table 1. Identification of chemical compositions of ES by GC and GC/MS

Chemical compositions	**Percentage (%)**
α-thujene	6.02
α-fenchone	0.10
Sabinene	0.13
β-pinene	0.18
Trans hydroxy oxide of linalool	0.29
1,8 cineole	73.10
(E)-β-ocimene	0.14
Camphenilone	0.14
Dehydro-linalool	0.42
2,6-dimehyl phenol	0.12
Trans-dihydro-β-terpineol	1.57
Camphre	0.07
β-oxide de pinene	0.21
Terpin-4-ol	0.45
α-terpineol	2.34
Formate de linalool	0.15
Citronellol	0.89
Piperonal	0.19
δ-elemene	0.97
Propanoate isobornyl	0.08
Sesquithujene	0.09
4,8-α-epoxy de caryophyllane	0.90
β-humulene	0.75
α-humulene	0.13
Sesquisabinene	0.32
α-isobutanoate de terpinyl	0.32
Trans-muurola-4(14),5-diene	1.86
Germacrene B	0.21
Alcool de caryophyllenyl	0.35
Spathulenol	0.38
Globulol	1.93
widdrol	1.39
Trans-β-elemenone	0.41
Citronellyl de pentanoate	0.46
γ-eudesmol	0.27
α-eudesmol	0.27

2.5. Scanning electron microscopic and energy dispersive spectroscopy analysis

The identification of the elements was analyzed by energy dispersive spectroscopy (EDS) and the image of the metal surface after the immersion time of 6 h, in the absence and the presence of an optimal concentration of ES were implicated by scanning electron microscopy (SEM) (JEOL JSM-IT 100/accelerating voltage 20 kV).

3. RESULTS AND DISCUSSION

3.1. Weight loss study

Several investigations examine the corrosion rate in different manners, but the weight loss method reports significant results that stimulate mass loss over time (Equation 1) [21–23].

$$C_R = \frac{m_i - m_f}{S \times t} \quad (1)$$

Where; C_R is the corrosion rate, the mass loss is expressed by the mass difference between the initial mass (m_i) and final mass (m_f), the substrate surface (S), and the immersion time (t). We have examined the behavior of the metal by this method with different concentrations of ES, and the results are listed in Table 2. Further, the evaluation of the efficiency of ES is treated through the following equation (2) [24,25]:

$$IE\ (\%) = \frac{C_{R_0} - C_{R_{inh}}}{C_{R_0}} \times 100 \quad (2)$$

Table 2. Effect of ES concentrations on corrosion rate

Quantity (g/L)	**0**	**0.1**	**0.6**	**1.8**	**2.4**
C_R ($mg.cm^{-2}.h^{-1}$)	0.237	0.098	0.079	0.063	0.051
IE (%)	-	58	66	73	78

The acquired results report a description of how the ES inhibitor influences the corrosion rate of the metal (Table 2), for all concentrations are assigned an efficiency greater than 50%, but less than 80%, which provides information that ES shows medium inhibition. Moreover, the same conditions were implanted with Eucalyptus Botryoides [20], and the published results exhibit an approving inhibition, which qualifies the effect of the chemical compositions of essential oil. In this study, the major compounds of ES essential oil are 1,8 cineole (73.10%), α-thujène (6.02%), and for another study, the main compounds of Eucalyptus Botryoides essential oil are α-pinene (55.16%), Trans-dihydro-α-terpineol (12.84%). From the point of view of chemical properties; this is one of the essential factors that contribute to affecting the mechanism of inhibition. Moreover, the theoretical view largely explains this behavior through the process of adsorption, in which the elements and the structure of the chemical compounds with the surface properties of the metal form the main aspects that contribute to defining the type of absorption process [26–28]. Another source of differentiation is competitive inhibition

and the influence of minor concentrations of other compositions which can control the effectiveness of inhibition through various issues.

3.2. Potentiodynamic polarization measurements

The current densities of the samples were recorded in different concentrations of ES depending on the applied polarization. Figure 1 shows that the effect of ES is more pronounced on the anodic sides of the potentiodynamic polarization curves, which affects the corrosion potential of the metal. The Tafel extrapolation was used to study this trend and the values of the parameters of the studied system were rearranged in Table 3.

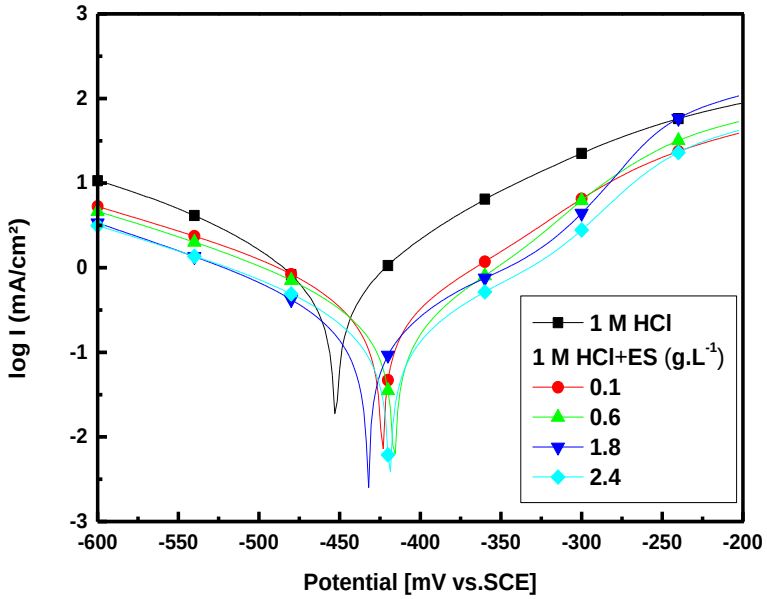

Figure 1. Effect of ES on C38 steel in 1 M HCl represented by polarization curves

From the results in Table 3, we notice that ES shifts the corrosion potential towards anodic potentials with a variation less than 85 mV, this behavior is interpreted by many authors, as a mixed inhibitors behavior [29–31]. Additionally, Figure 1 shows that anodic branches are more affected than cathodic branches. According to Table 3, the anodic slopes change remarkably in the presence of ES. This significant change may result, that ES chemical compositions preferring anodic active sites on the metal surface. Moreover, the anodic slopes of Tafel are reduced to values below 108.2 mV/dec, which may indicate the participation of ES chemical compositions in the anodic kinetics of iron dissolution, due to the predominant effect of ES when its concentration increases [32]. This behavior can be validated by anodic potentiodynamic polarization curves (Figure 1), after the first iron dissolution, a delay in the anodic kinetics is observed compared to a solution containing just HCl, then after the potential of about -325 mV/SCE, a remarkable acceleration of anodic kinetics is evoked and interpreted by many authors as a result of the desorption process [33–35]. On the other hand, the cathodic

Tafel slope values are around 120 mV/dec, which means that the charge transfer mechanism controlling the hydrogen reduction reaction remained unchanged in the presence of ES [36,37].

Table 3. Impact of ES on the electrochemical parameters of steel C38 in 1 M HCl

Quantity ($g\ L^{-1}$)	$-E_{corr}$ ($mV.SCE^{-1}$)	i_{corr} ($\mu A\ cm^{-2}$)	$-\beta_c$ ($mV\ dec^{-1}$)	β_a ($mV\ dec^{-1}$)	**E (%)**
0	452	787.6	125.7	108.2	-
0.1	422	299.5	131.2	96.0	62
0.6	414	234.0	130.1	84.2	70
1.8	430	202.0	129.7	79.8	74
2.4	417	149.3	124.4	83.3	81

Furthermore, the current density is decreased, which shows 81% corrosion inhibition efficiency at the maximum concentration of ES (Table 3), this behavior means that the process of adsorption of ES compositions does not reveal a good behavior at the surface of the material. In addition, organic inhibitors are known to be good acid corrosion inhibitors [38–41], which adsorb to metal surfaces by different adsorption mechanisms. Since ES has complex compositions, the appropriate adsorption mechanism can be difficult to set up [42]. On the other hand, 1,8-cineole is the majority constituent of ES which represents 73% (Table 1); Its adsorption may be excluded by other compounds of essential oil or its inhibition behavior is insufficient. In our previous research [20], Eucalyptus Botryoides oil, which contains 55% α-pinene and 12% trans-dihydro-α-terpineol, showed high corrosion inhibition efficiency of about 93% at the maximum concentration, which means that the main constituents act an important role in the inhibitory action of the essential oil.

3.3. Electrochemical impedance spectroscopy (EIS)

The EIS technique has been massively used by many researchers. Figure 2 shows impedance curves collected as Nyquist plots, describing a capacitive behavior that relates the corrosion process to the charge transfer mechanism [43,44], This behavior has been cited by several authors, and the main influences on this situation are the nature of the surface, and the compositions of the solution [45], as well as other authors, who have cited the adsorption effect of the intermediate product [46,47]. In addition, ES increases the real and imaginary impedance which increases the diameter of the semicircle of the Nyquist plots, therefore, ES lowers the charge transfer process; and the protection of the metal is improved.

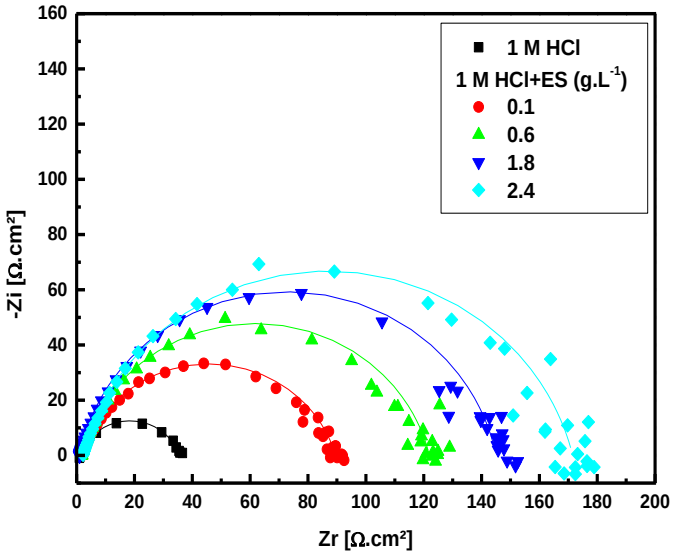

Figure 2. Impact of ES on the Nyquist plots of steel C38 in 1 M HCl

Moreover, the appropriate data was acquired by selecting the accurate electrical equivalent circuit that illustrates the special progression of the metal/solution interface (Figure 3). This circuit describes the capacitance behavior using the constant phase element (CPE) and the resistance of metal via the charge transfer resistance (R_{ct}), and the degree of conductivity of the solution by the electrolyte resistance (R_s). In general, the charge transfer resistance and the double-layer capacitance C_{dl} are connected in parallel to explain the corrosion process.

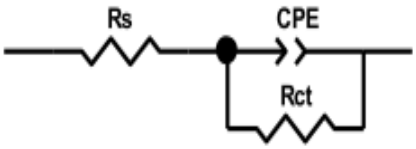

Figure 3. Electrical equivalent circuit showing the progression of the metal/solution interface

The calculated impedance of CPE is described using this relation [41,48,49]:

$$Z_{CPE} = \frac{1}{Y_0(j\omega)^n} \quad (3)$$

The degree of CPE and phase shift is designed by Yo and n, respectively, and ω represents the angular frequency, the double-layer capacitance C_{dl} is estimated through equation (4) [50]. The parameters of the model are organized in Table 4.

$$C_{dl} = \left(Y_0^{\frac{1}{n}}(R_{ct})^{\frac{1-n}{n}}\right) \quad (4)$$

The model fitting results confirm the ability of ES to negatively affect charge transfer and double-layer capacitance with increasing ES concentration, and a similar behavior appears for the inhibition efficiency which is estimated from the following equation (5) [51,52]:

$$E\ (\%) = \frac{R_{ct} - R_{ct}^{0}}{R_{ct}} \times 100 \quad (5)$$

Where the charge transfer resistance values R_{ct}^{0} and R_{ct} without and with the ES, respectively.

Table 4. Electrochemical impedance parameters of the model in the presence of different concentrations of ES

Quantity ($g.L^{-1}$)	R_s ($\Omega\ cm^2$)	Y_0 ($\mu\Omega^{-1}\ s^n\ cm^2$)	**n**	R_{ct} ($\Omega\ cm^2$)	C_{dl} ($\mu F/cm^2$)	**E (%)**
Blank	1.22	314	0.821	33.97	116.80	-
0.1	2.04	239	0.825	87.51	105.30	61
0.6	1.68	175	0.855	120.30	90.95	72
1.8	0.89	148	0.876	144.10	86.17	76
2.4	2.19	132	0.880	169.40	78.88	80

In addition, the effectiveness of 0.1 g/L and 2.4 g/L represents 61% and 80% respectively, which means that the ES compositions created a defensive barrier to protect the metal. The nature of the protection depends essentially on the type of interaction that occurs between the ES compounds and the metal surface, and on the nature of the aggressive solutions. Regardless of the type of reaction, many parameters affect the resistance of the metal to corrosion, such as the nature of the oxide layer and the relative contact of the metal surface with the corrosion solution. For this, the increase in efficiency could be related to the modification of these parameters, especially since the efficiency depends on the ES concentration. On the other hand, we noticed that the efficiency remained between 60% and 80% even though we changed the concentration from 0.1 g/L to 2.4 g/L, which means that the ES does not show high efficiency. This behavior may depend on the chemical compositions of ES, the nature of the solution, and the surface of the metal.

Generally, the effect of essential oils on corrosion protection is due to their chemical compositions, which include different categories of compounds such as terpenes, phenols, aldehydes, and ketones, and the mechanism by which these chemicals exercise their anti-corrosion effect is not fully understood. However, it is believed that the active compounds of essential oils form a protective layer on the surface of the metal, preventing corrosive agents from contacting the metal.

3.4. Temperature effect

The ability of ES to resist temperature modification at optimum inhibition concentration was examined (2.4 g/L) via EIS measurements (Figure 4). As shown in this figure, higher

temperatures weaken the resistance of the metal; however, the presence of ES maintains the resistance of the metal to the aggressive solution. On the other hand, the behavior of the metallic surface preserves the capacitive demeanor which is a sign that charge transfer is still the dominant mechanism.

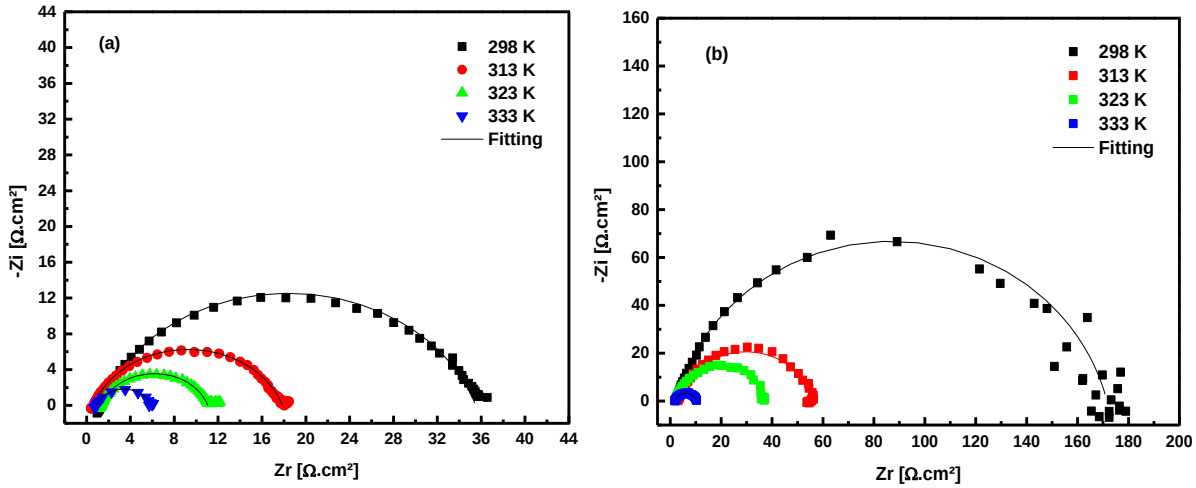

Figure 4. Impact of temperature modification on the Nyquist plots of steel C38 in (a) 1 M HCl (b) 1 M HCl with 2.4 g/L of ES

Moreover, Table 5 lists the model parameters extracted using the previous equivalent electrical circuit (Figure 4). As revealed, the charge transfer resistance in the presence of ES shows higher values compared to the blank solution, which means that the ES reduces the influence of temperature, as a result of which reduces the degradation of the metal.

Table 5. Impact of temperature modification on the electrochemical impedance parameters of C38 steel in 1 M HCl and at optimum inhibition concentration of ES

	Temperature	**R_s (Ω cm^2)**	**Y_0 ($\mu\Omega^{-1}$ s^n cm^2)**	**n**	**R_{ct} (Ω cm^2)**	**C_{dl} (μF/cm^2)**	**i_{cor} (mA cm^{-2})**	**E (%)**
Blank	298	1.22	3.14	0.821	33.97	116.80	0.378	-
	313	0.57	4.84	0.813	17.05	160.00	0.791	-
	323	1.26	5.63	0.800	9.86	155.00	1.411	-
	333	0.85	7.42	0.804	5.07	189.40	2.830	-
ES	298	2.19	1.51	0.850	169.40	78.88	0.0757	80
	313	3.03	2.55	0.837	53.49	110.60	0.252	68
	323	1.87	2.33	0.842	36.11	95.19	0.385	73
	333	1.83	5.24	0.811	8.75	148.9	1.640	42

This is illustrated in the estimated corrosion inhibition efficiency, as displayed in Table 5, the efficiency is less than 80% at different temperatures and becomes less than 50% at 333 K, and this reduced value may be related to the physisorption process. Besides, the type of inhibitor plays a vital role in preventing metal corrosion in such an environment, for example in an acidic medium, organic inhibitors are the main answer to reduce the corrosion rate [28,53–56], whose molecular structures and structural properties influence the effectiveness of inhibition. In our case, the ineffectiveness of the inhibition at high temperatures indicates poor adsorption of ES compounds on the metal surface.

For thermodynamic investigation, the charge transfer resistance (R_{ct}) is converted to the corrosion current density (i_{corr}) using the following equation [33]:

$$i_{corr} = \frac{RT}{zFR_{ct}} \quad (6)$$

Where T is the temperature represented in Kelvin, and R represents the universal gas constant (8.314 J $K^{-1}mol^{-1}$). And for the valence z is replaced by 2 to express the valence of iron, and F is Faraday's constant (96 485 C). By this parameter, the Arrhenius and transition-state plots of C38 steel are plotted (Figure 5), the thermodynamic parameters of C38 steel in 1 M HCl and at optimum inhibition concentration of ES are obtained from equations (7) and (8) [57,58].

$$i_{corr} = Kexp(\frac{-E_a}{RT}) \quad (7)$$

$$i_{corr} = \frac{RT}{Nh}\exp\left(\frac{\Delta S_a}{R}\right)\exp\left(\frac{-\Delta H_a}{RT}\right) \quad (8)$$

Where, the constant parameters N, K, h represent the Avogadro's number (6.022×10^{23} mol^{-1}), Arrhenius pre-exponential factor, Plank's constant (6.6261×10^{-34}J s) respectively, $E_a$is the activation energy, ΔH_a represents the enthalpy of the reaction, and ΔS_a describes the entropy of the system.

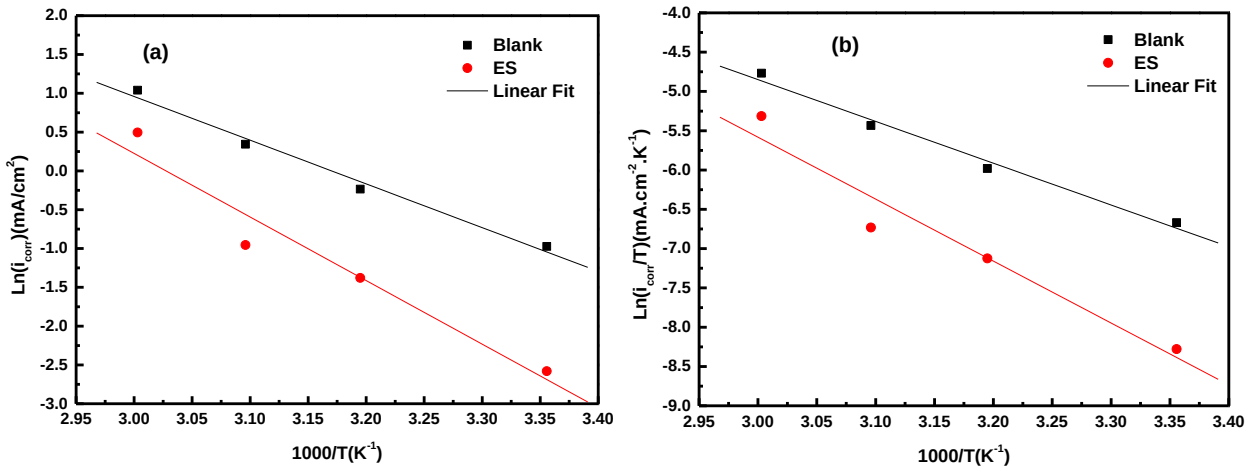

Figure 5. Effect 2.4 g/L of ES on (a) the Arrhenius and (b) transition-state plots of steel C38 in 1 M HCl

Table 6 shows the effect of ES on thermodynamic parameters, the results reveal that ES improves E_a, ΔH_a, ΔS_a. Moreover, regarding the corrosion process of the system, the ES increases the activated energy and preserves the endothermic nature of the system, with this change; the disorder of the system is developed into a high value.

Table 6. Effect of ES on the thermodynamic parameters

Thermodynamic parameters	**ΔS_a (J/K mol)**	**ΔH_a (kJ/mol)**	**E_a (kJ/mol)**
1 M HCl	-105.22	44.21	46.83
2.4 g/L	-47.42	65.51	68.13

3.5. Surface studies

Special resolution and analytical imaging using SEM have been exploited to produce data that can prove ES performance. The technique was carried out on the surfaces of the sample after a considered time of 6 hours, depending on the presence of ES (Figure 6). The qualitative evaluation of the images shows severe degradation of the metal indicating that the aggressive solution damages the sample surface (Figure 6a). On the other hand, Figure 6b reveals the effect of ES on the surface of the substrate, and this picture exhibits less surface degradation which indicates the protection of the metal. This modification may be due to the effect of ES on the thermodynamic parameters of the reactions that occur on the metal surface. Furthermore, quantitative evaluation of surface structures provides essential data on how ES protects the metal surface (Table 7). It is noted that the mass ratios of oxygen and iron differ in both cases, and they decrease in the case where ES is present in the solution. This corresponds to the state of the metal surface and the results of the electrochemical analysis.

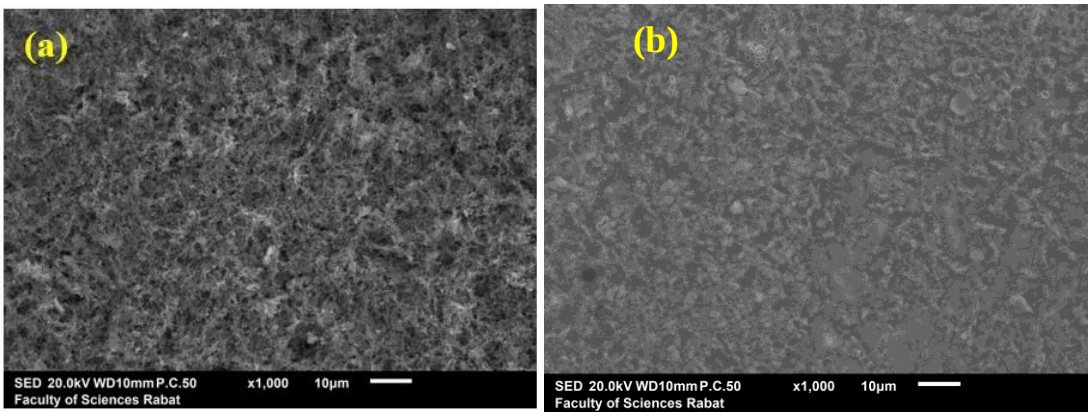

Figure 6. C38 steel surface after 6 h of immersion (a) in 1 M HCl (b) in 1 M HCl + 2.4 g/L of ES

Table 7. Quantitative effect of 2.4 g/L of ES on the surface compositions of the C38 steel in 1 M HCl after 6 h of immersion

Mass (%)	**1 M HCl**	**2.4 g/L**
Fe	74.91	68.94
O	18.15	12.84
C	5.59	2.69
Cl	0.3	14.77
N	-	0.76

4. CONCLUSION

Eucalyptus Sideroxylon essential oil is being studied to exploit its corrosion inhibition potential to protect C38 steel in an acid solution of HCl (1M) via a variety of technologies and methods for example SEM/EDS, weight loss, and electrochemical investigations. A weight loss study showed that ES compositions reduce metal corrosion rate for all concentrations and the effectiveness is determined between 50% and 80%. PDP explained that the ES compositions change the corrosion potential towards anodic potentials below 85 mV, preferring to inhibit the anodic reactions on the metal surface and preserve the charge transfer mechanism that controls the hydrogen reduction reaction. EIS using Nyquist plots showed capacitive behavior in the absence and presence of ES compositions, meaning that the corrosion process is controlled by the charge transfer mechanism and metal impedance obtain high values in the presence of ES compositions. These values decrease under the influence of temperature, which allows us to relate this behavior to the process of physisorption. The effect of ES on thermodynamic parameters is also studied, and the results reveal that ES improves. SEM exposed the consequence of the presence of ES on the metal surface, indicating the protection of the metal. Finally, we noticed that the ES does not show a high efficacy compared to the previous study of Eucalyptus Botryoides oil, which means that the main constituents play an important role in the inhibitory action of the essential oil.

Acknowledgments

We thank all colleagues.

Declarations of interest

The authors declare no conflict of interest in this reported work.

REFERENCES

[1] M. Sabouri, T. Shahrabi, H.R. Faridi, and M. Salasi, Corros. Eng. Sci. Technol. 44 (2009) 51.

[2] M. Belayachi, H. Serrar, H. Zarrok, A. El Assyry, A. Zarrouk, H. Oudda, S. Boukhris, B. Hammouti, Eno E. Ebenso, and A. Geunbour, Int. J. Electrochem. Sci. 10 (2015) 3010.

[3] H. Tayebi, H. Bourazmi, B. Himmi, A. El Assyry, Y. Ramli, A. Zarrouk, A. Geunbour, B. Hammouti, and Eno E. Ebenso, Der Pharmacia Lett. 6 (2014) 20.

[4] A. Zarrouk, H. Zarrok, R. Salghi, N. Bouroumane, B. Hammouti, S. S. Al-Deyab, and R. Touzani, Int. J. Electrochem. Sci. 7 (2012) 10215.

[5] H. Zarrok, K. Al Mamari, A. Zarrouk, R. Salghi, B. Hammouti, S. S. Al-Deyab, E. M. Essassi, F. Bentiss, and H. Oudda, Int. J. Electrochem. Sci. 7 (2012) 10338.

[6] H. Tayebi, H. Bourazmi, B. Himmi, A. El Assyry, Y. Ramli, A. Zarrouk, A. Geunbour, and B. Hammouti, Der Pharma Chem. 6 (2014) 220.

[7] A. Zarrouk, H. Zarrok, R. Salghi, R. Touir, B. Hammouti, N. Benchat, L. L. Afrine, H. Hannache, M. El Hezzat, and M. Bouachrine, J. Chem. Pharm. Res. 5 (2013) 1482.

[8] H. Zarrok, A. Zarrouk, R. Salghi, M. Ebn Touhami, H. Oudda, B. Hammouti, R. Touir, F. Bentiss, and S. S. Al-Deyab, Int. J. Electrochem. Sci. 8 (2013) 6014.

[9] H. Zarrok, R. Salghi, A. Zarrouk, B. Hammouti, H. Oudda, Lh. Bazzi, L. Bammou, and S. S. Al-Deyab, Der Pharma Chem. 4 (2012) 407.

[10] Z. Tao, W. He, S. Wang, S. Zhang, and G. Zhou, J. Mater. Eng. Perform. 22 (2013) 774.

[11] S.M.Z. Hossain, S.A. Razzak, and M.M. Hossain, Arab. J. Sci. Eng. 45 (2020) 7137.

[12] M. Znini, Arab. J. Med. Aromat. Plants. 5 (2019) 1.

[13] L. De Martino, V. De Feo, and F. Nazzaro, Molecule 14 (2009) 4213.

[14] N.G. Chorianopoulos, E.D. Giaouris, P.N. Skandamis, S.A. Haroutounian, and G.J.E. Nychas, J. Appl. Microbiol. 104 (2008) 1586.

[15] S.A. Burt, and R.D. Reinders, Lett. Appl. Microbiol. 36 (2003) 162.

[16] F. Nazzaro, F. Fratianni, L. De Martino, R. Coppola, and V. De Feo, Pharmaceuticals 6 (2013) 1451.

[17] R. Idouhli, A. Oukhrib, M. Khadiri, O. Zakir, A. Aityoub, A. Abouelfida, A. Benharref, and A. Benyaich, J. Mol. Struct. 1228 (2021) 129478.

[18] K. Dahmani, M. Galai, M. Ouakki, M. Cherkaoui, R. Touir, S. Erkan, S. Kaya, and B. El Ibrahimi, Inorg. Chem. Commun. 124 (2021) 108409.

[19] A. Chraka, I. Raissouni, N. Benseddik, S. Khayar, A. Ibn Mansour, H. Belcadi, F. Chaouket, and D. Bouchta, Mater. Today Proc. 22 (2020) 83.

[20] L. Koursaoui, Y. Kerroum, M. Tabyaoui, A. Guenbour, A. Bellaouchou, B. Satrani, M. Ghanmi, I. Warad, A. Chaouch, and A. Zarrouk, Biointerface Res. Appl. Chem. 11 (2021)

10119.

[21] A. Zarrouk, H. Zarrok, R. Salghi, R. Touir, B. Hammouti, N. Benchat, L.L. Afrine, H. Hannache, M. El Hezzat, and M. Bouachrine, J. Chem. Pharm. Res. (2013) 1482.

[22] C. Cuevas-Arteaga, J. Uruchurtu-Chavarín, J. Porcayo-Calderon, G. Izquierdo-Montalvo, and J. Gonzalez, Corros. Sci. 46 (2004) 2663.

[23] N.O. Obi-Egbedi, K.E. Essien, I.B. Obot, and E.E. Ebenso, Int. J. Electrochem. Sci. 6 (2011) 913.

[24] X. Li, and G. Mu, Appl. Surf. Sci. 252 (2005) 1254.

[25] M. Dahmani, A. Et-Touhami, S.S. Al-Deyab, B. Hammouti, and A. Bouyanzer, Int. J. Electrochem. Sci. 5 (2010) 1060.

[26] A. Dutta, S.K. Saha, P. Banerjee, A.K. Patra, and D. Sukul, RSC Adv. 6 (2016) 74833.

[27] J. Zhang, X.L. Gong, H.H. Yu, and M. Du, Corros. Sci. 53 (2011) 3324.

[28] M. Athar, H. Ali, and M.A. Quraishi, Br. Corros. J. 37 (2002) 155.

[29] M. Behpour, S.M. Ghoreishi, M. Salavati-Niasari, and N. Mohammadi, JNS 2 (2012) 317.

[30] A. Zhao, H. Sun, L. Chen, Y. Huang, X. Lu, B. Mu, H. Gao, S. Wang, and A. Singh, Int. J. Electrochem. Sci. 14 (2019) 6814.

[31] R. Hsissou, S. Abbout, R. Seghiri, M. Rehioui, A. Berisha, H. Erramli, M. Assouag, and A. Elharfi, J. Mater. Res. Technol. 9 (2020) 2691.

[32] Z. Zeng, R.S. Lillard, and H. Cong, Corrosion. 72 (2016) 805.

[33] M. El Faydy, R. Touir, M. Ebn Touhami, A. Zarrouk, C. Jama, B. Lakhrissi, L.O. Olasunkanmi, E.E. Ebenso, and F. Bentiss, Phys. Chem. Chem. Phys. 20 (2018) 20167.

[34] N.C. Ngobiri, E.E. Oguzie, N.C. Oforka, and O. Akaranta, Arab. J. Chem. 12 (2019) 1024.

[35] S.A. Umoren, M.M. Solomon, Prog. Mater. Sci. 104 (2019) 380.

[36] K. Jüttner, Mater. Corros. Korrosion, 31 (1980) 358.

[37] T. Shinagawa, A.T. Garcia-Esparza, and K. Takanabe, Sci. Rep. 5 (2015) 1.

[38] E. Kamali Ardakani, E. Kowsari, and A. Ehsani, Colloids Surfaces A 586 (2020) 124195.

[39] M.A. Deyab, M.T. Zaky, and M.I. Nessim, J. Mol. Liq. 229 (2017) 396.

[40] S. Rajendraprasad, S. Ali, and B.M. Prasanna, J. Fail. Anal. Prev. 20 (2020) 235.

[41] T. Yan, S. Zhang, L. Feng, Y. Qiang, L. Lu, D. Fu, Y. Wen, J. Chen, W. Li, and B. Tan, J. Taiwan Inst. Chem. Eng. 106 (2020) 118.

[42] S. Lyubchik, A. Lyubchik, O. Lygina, S. Lyubchik, and I. Fonsec, Thermodynamics-Interaction Studies - Solids, Liquids and Gases, InTech (2011).

[43] M. El Faydy, B. Lakhrissi, C. Jama, A. Zarrouk, L.O. Olasunkanmi, E.E. Ebenso, and F. Bentiss, J. Mater. Res. Technol. 9 (2020) 727.

[44] A. Batah, A. Anejjar, L. Bammou, M. Belkhaouda, and R. Salghi, Port. Electrochim. Acta 38 (2020) 201.

[45] A. Singh, K.R. Ansari, D.S. Chauhan, M.A. Quraishi, H. Lgaz, and I.M. Chung, J. Colloid Interface Sci. 560 (2020) 225.
[46] Y. Kerroum, A. Guenbour, A. Bellaouchou, H. Idrissi, J. García-Antón, and A. Zarrouk, Anal. Bioanal. Electrochem. 11 (2019) 497.
[47] Z. Salarvand, M. Amirnasr, M. Talebian, K. Raeissi, and S. Meghdadi, Corros. Sci. 114 (2017) 133.
[48] D. Li, D. Chen, J. Wang, and H. Chen, Acta Metall. Sin. (Engl. Lett.) 23 (2010) 461.
[49] A. El Guerraf, A. Titi, K. Cherrak, N. Mechbal, M. El Azzouzi, R. Touzani, B. Hammouti, and H. Lgaz, Surfaces and Interfaces 13 (2018) 168.
[50] Y. Kerroum, A. Guenbour, A. Bellaouchou, H. Idrissi, J. Garcia-Anton, and A. Zarrouk, J. Bio-Tribo-Corrosion. 5 (2019) 68.
[51] Y. Meng, W. Ning, B. Xu, W. Yang, K. Zhang, Y. Chen, L. Li, X. Liu, J. Zheng, and Y. Zhang, RSC Advances 7 (2017) 43014.
[52] V.C. Anadebe, O.D. Onukwuli, M. Omotioma, and N.A. Okafor, Mater. Chem. Phys. 233 (2019) 120.
[53] E. Alibakhshi, M. Ramezanzadeh, G. Bahlakeh, B. Ramezanzadeh, M. Mahdavian, and M. Motamedi, J. Mol. Liq. 255 (2018) 185.
[54] A. Zarrouk, B. Hammouti, T. Lakhlifi, M. Traisnel, H. Vezin, and F. Bentiss, Corros. Sci. 90 (2015) 572.
[55] I. Elazhary, M.R. Laamari, A. Boutouil, L. Bahsis, M. El Haddad, H. Anane, and S.E. Stiriba, Anti-Corrosion Methods Mater. 66 (2019) 544.
[56] C. Verma, and M.A. Quraishi, Org. Corros. Inhib. (2021) 149.
[57] M. Boudalia, A. Bellaouchou, A. Guenbour, H. Bourazmi, M. Tabiyaoui, M. El Fal, Y. Ramli, E. Mokhtar Essassi, and H. Elmsellem, J. Chem. 2 (2014) 97.
[58] H. Bourazmi, M. Tabyaoui, L. El Hattabi, Y. El Aoufir, and M. Taleb, J. Mater. Environ. Sci. 9 (2018) 928.